Robust Fault-Tolerant Control of an Electro-Hydraulic Actuator With a Novel Nonlinear Unknown Input Observer

VAN DU PHAN[ID]**, CONG PHAT VO**[ID]**, HOANG VU DAO**[ID]**, AND KYOUNG KWAN AHN**[ID]**, (Senior Member, IEEE)**

School of Mechanical and Automotive Engineering, University of Ulsan, Ulsan 44610, South Korea

Corresponding author: Kyoung Kwan Ahn (kkahn@ulsan.ac.kr)

ABSTRACT In this paper, a novel adaptive fault-tolerant controller is proposed for a typical electro-hydraulic rotary actuator in the presence of disturbances, internal leakage fault, and sensor fault simultaneously. To construct the suggested controller, a nonlinear unknown input observer is developed to effectively identify the sensor fault, which is unaffected by not only internal leakage fault but also mismatched disturbances/uncertainties. Furthermore, a radial basis function neural network is designed to compensate for the mismatched disturbances/uncertainties caused by payload variation and unknown friction nonlinearities. Besides, an adaptive law based on the projection mapping function is applied to tackle the effect of the internal leakage fault. The integration of the above-mentioned techniques into the adaptive backstepping terminal sliding mode is investigated to obtain high tracking performance, robustness as well as fast convergence. The stability of the closed-loop system is proven by the Lyapunov theory. Finally, the capability and effectiveness of the proposed approach are validated via simulation results under various faulty scenarios.

INDEX TERMS Mismatched disturbance, fault detection and identification, fault-tolerant control.

I. INTRODUCTION

Nowadays, with the development of modern industrials, the hydraulic actuator has been the most popular and widely used in many applications such as robotic manipulators, ships, aerospace systems. Although this actuator has outstanding advantages of a high-power-to-weight ratio, high accuracy, cost, and fast response, the model uncertainty is a big challenge in ensuring operational efficiency. In detail, the hydraulic system always exists parametric uncertainties, external disturbance, and unmodeled nonlinearities as well as faults [1]–[4]. In order to improve the system performance, the disturbance is not only needfully suppressed but also compensated by assisted techniques such as extended state observer [5], [6], neural network (NN) approximators [7]–[10] fuzzy logic system (FLS) [11], time-delay estimation (TDE) [12], [13], etc. In a certain way, the disturbances or uncertainties can be considered as faults,

The associate editor coordinating the review of this manuscript and approving it for publication was Hao Luo[ID].

which seriously affect system performance and safety [14]. In an electro-hydraulic actuator (EHA), the possible faults have normally happened relating to the mechanism, electronic amplifiers, servo valves, hydraulic cylinders, sensor components, or power supply with different features [3]. For the closed-loop control in complex systems such as aircraft, construction machines, automobiles, serious accidents may occur due to system fault. Hence, the fault-tolerant controller (FTC) is developed to deal with the impact of faults on the system which can be classified into two main types [15]: sensor fault and actuator fault.

In the engineering system, a measurement part plays an especially key role in the tracking control. For instance, the sensor fault could be happened in position sensors, pressure sensors, load cells in the hydraulic robot [16], in generators and rotor speed sensors of a wind turbine [17], in the sensor measuring jacket temperature of chemical plants [18], and on voltage sensors, current sensors and speed sensor of the electrical traction system [19], etc. Thus, any sensor fault occurs in the overall system that can affect significantly tracking

performance [20], [21]. Inspired by fault estimation techniques, the alarm system failures and the suitable acts are decided as soon as possible to avoid heavy damages and dangerous situations. The idea of fault detection and identification (FDI) method becomes a powerful tool to reach the information of a sensor fault as well as an actuator fault [22]–[25]. In order to deploy the mentioned aim, several observer strategies have been investigated to estimate sensor faults such as adaptive observer [26]–[28], extended Kalman filter [29], [30], and Takagi-Sugeno fuzzy observer [17], [31]. Especially, an unknown input observer (UIO) is not only an accurate estimation but also a helpful method to distinguish disturbances and faults. It had thus become increasingly popular in the last decade in which observer gain is designed based on the linear matrix inequality (LMI) optimization algorithm [32]–[34]. In [35], the sensor faults including position and pressure with noise have been presented for EHA, then an UIO-integrated extended finite impulse response (EFIR) has been investigated to determine the sensor fault but the actuator fault has not been carried out. Meanwhile, a robust nonlinear unknown input observer (NUIO) [18] has been also designed to detect only sensor fault without fault estimation. It has been applied to a continuous stirred tank reactor with respect to external disturbances. Furthermore, a higher-order sliding mode observer [36] has been proposed to regulate the vehicle speed in the event of sensor faults/failures. Nevertheless, the effect of the disturbance has not been completely resolved yet. The common advantage of those methods is that they provide a valuable and uncomplicated design strategy to preserve an acceptable system performance in presence of sensor faults and with/without disturbances. Besides sensor faults, another popular reason affecting control effectiveness is caused by actuator faults, especially the internal leakage fault.

From the actuator fault perspective, many recent studies determined actuator fault as loss-of-effectiveness faults or lumped unknown components [37]–[39]. In [40], [41] an internal leakage fault under the model uncertainties/time-varying load has been accommodated via the adaptive parameter estimation. Then, the control performance has been recovered by the FTC when the fault had been detected through the available sensor measurements. In another study, the actuator internal leakage and valve spool blockage are diagnosed by the NN without the presence of disturbances or sensor faults. Because the linearized model is used, it reduces the inherent nonlinearity of the system [42]. In [43], the position controller is tolerant with actuator internal leakage and robust with parametric uncertainties in the EHA in which the sensor fault is not considered. Different techniques like wavelet transform [44], Hilbert-Huang transform [45] have been applied to reduce the effects of the actuator fault. However, these techniques approach for FTC in general have not clearly analyzed the decoupling between actuator fault and disturbances/uncertainty. Consequently, it is worth pointing out that most of all the above-mentioned methods are to construct a fault estimation effective for sensor or actuator

fault which helps to improve the safety and reliability as well as the control performance of the system.

As the above analysis literature, most of the previous studies only considered either the sensor fault or the actuator fault with/without disturbances for tracking control problem. However, it is noteworthy that in the practical hydraulic system, phenomena as mismatched disturbances, sensor faults, and actuator faults may happen simultaneously. Therefore, the FDI and FTC developments are important to ensure the safety and reliability of the hydraulic control system, especially, in the presence of concerned faults and mismatched disturbances. This approach combines the FTC technique-assisted the fault information of FDI, called active FTC [46], [47]. Hence, to overcome these aforementioned drawbacks, in this work, an active FTC is proposed for an electro-hydraulic rotary actuator (EHRA) based on a novel NUIO and adaptive control laws. In detail, the NUIO is designed based on the LMI approach to estimate the position sensor fault under the effect of actuator faults and disturbances. Then, the fault detection (FD) performs the comparative duty of the fault estimation with a determined threshold, which is decided via [35], [48]. Next, the feedback position signal at the principal controller is obtained by the estimated values instead of the measured value when the fault exceeds the predefined threshold in real-time. Moreover, the radius bias function neural network (RBFNN) approximator and the projection adaptive law are integrated into the proposed control scheme to handle both actuator faults and mismatched disturbances. Finally, an adaptive backstepping terminal sliding mode controller (ABTSMC) [49]–[51] is proposed to enhance the robustness with uncertainties and approximation error. The proposed active FTC not only ensure the stability of the controlled system but also maintain acceptable control performances in the presence of faulty conditions. Compared with existing works, the main contributions of this paper can be shown as follows:

- According to the author's knowledge, a novel active FTC approach is firstly proposed for EHRA in the presence of the mismatched disturbances, internal leakage, and sensor faults, simultaneously.
- The novel NUIO-based FDI scheme is designed to take part in estimating the system states, detecting and identifying the sensor fault under the influences of internal leakage fault, and mismatched disturbances.
- The stability of the closed-loop system is proven by the Lyapunov theory with the assist of an extended Barbalat's Lemma. Additionally, the effectiveness of proposed control approach is verified in various simulation conditions.

The remainder of this paper is organized as the following: In section II, the system model of the EHRA and the main objectives are described. Section III proves the FDI method and proposes a novel active FTC. Section IV presents the simulation results. Lastly, the conclusions and future works are expressed in Section V.
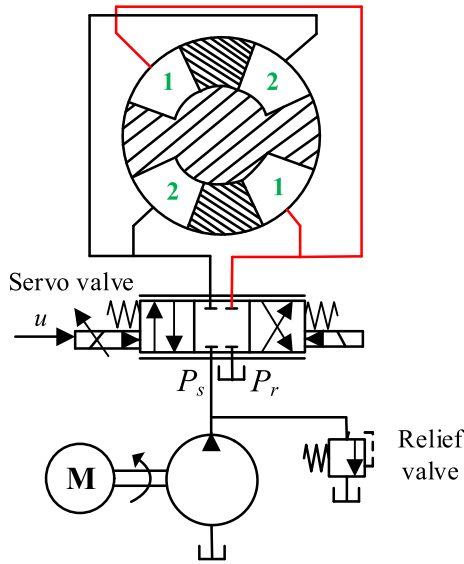
FIGURE 1. Architecture of electro-hydraulic rotary actuator.

II. HYDRAULIC ROTARY SYSTEM MODELING WITH FAULT

The structure of the EHRA is described in Fig. 1. The control signal from the controller is supplied to the servo-valve, which regulates the flow rates and pressures in both chambers of the rotary actuator. Hence, the inertial load is controlled to track a reference trajectory. The sensor system is set up to measure the rotational angle, rotational speed, and pressure of both chambers. These signals are feedback to the controller, which completes the closed-loop system design.

The mechanical dynamics is presented as

$$J\ddot{q} = P_L A - B\dot{q} + d_m(t, q, \dot{q}) \qquad (1)$$

where q, J, and B represent the angular displacement, inertia moment, and viscous damping coefficient, respectively; $d_m(\bullet)$ is a lumped disturbance/uncertainty term, which t and $\dot{q}$ are assumed to depend on time and angular velocity, P_L denotes the load pressure which is computed as the following.

$$P_L = P_1 - P_2 \qquad (2)$$

where P_i is the pressure value of ith chamber ($i = 1, 2$).

The pressure dynamics of both chambers are expressed by [2], [4], [5]

$$\dot{P}_1 = \frac{\beta_e}{V_1}(-A\dot{q} - q_L + Q_1)$$

$$\dot{P}_2 = \frac{\beta_e}{V_2}(A\dot{q} + q_L - Q_2) \qquad (3)$$

where β_e, A and q_L are the Bulk modulus, a ram area, and the internal leakage, respectively. $V_1 = V_{01} + Aq$ and $V_2 = V_{02} + Aq$ are the trapped volumes of both sides of the actuator and V_{01}, V_{02} are the initial values. Q_1 and Q_2 are the flowrate go into 1st chamber and the flow-rate go from the 2nd chamber, which are described by the equations below.

$$Q_1 = k_t u\left[s(u)\sqrt{P_s - P_1} + s(-u)\sqrt{P_1 - P_r}\right]$$

$$Q_2 = k_t u\left[s(u)\sqrt{P_2 - P_r} + s(-u)\sqrt{P_s - P_2}\right] \qquad (4)$$

where P_s and P_r are the supply pressure and return pressure, k_t is a proportional gain of the servo-valve, u is the control voltage generated by the controller, and $s(u)$ is defined as

$$s(u) = \begin{cases} 1, & \text{if } u \geq 0 \\ 0, & \text{if } u < 0 \end{cases} \qquad (5)$$

The fault is considered in this work including position sensor fault and leakage fault because they show serious failures and usually happen in the hydraulic control system. When the internal leakage fault occurs, it can be described as [40]

$$q_L = C_0(P_1 - P_2) + C_t\sqrt{|P_1 - P_2|}\text{sign}(P_1 - P_2) \qquad (6)$$

where C_0 is the nominal coefficient of the internal leakage of the rotary actuator; C_t is the internal leakage fault coefficient.

When the position sensor fault occurs, the measured angular displacement q is replaced by $q + f_s$. In this paper, it is assumed that the position sensor fault f_s is generated by a process with an unknown input signal ζ as below [29], [35].

$$\dot{f}_s = -k_s f_s + \zeta \qquad (7)$$

Define the state variables $x = [x_1, x_2, x_3, x_4]^T := [q, \dot{q}, AP_L/J, f_s]^T$. From (1)–(7), the total system is given as

$$\begin{cases} \dot{x}_1 = x_2 \\ \dot{x}_2 = x_3 + h(x_2) + d(x_1, x_2, t) \\ \dot{x}_3 = f(x_1, x_2, x_3) + g(x_1)u + f_a(x_1, x_3, t) \\ \dot{x}_4 = -k_s x_4 + \zeta \\ y = Cx \end{cases} \qquad (8)$$

where

$$h(x_2) = -\frac{Bx_2}{J}, \quad g(x_1) = \frac{\beta_e k_t A}{J}\left(\frac{R_1}{V_1} + \frac{R_2}{V_2}\right),$$

$$f(x_1, x_2, x_3) = -\left(\frac{\beta_e A^2 x_2}{J} + C_0 \beta_e x_3\right)\left(\frac{1}{V_1} + \frac{1}{V_2}\right),$$

$$R_1 = s(u)\sqrt{P_s - P_1} + s(-u)\sqrt{P_1 - P_r},$$

$$R_2 = s(u)\sqrt{P_2 - P_r} + s(-u)\sqrt{P_s - P_2},$$

$$d(x_1, x_2, t) = \frac{d_m(x_1, x_2, t)}{J}, \quad C = \begin{bmatrix} 1 & 0 & 0 & 1 \\ 0 & 1 & 0 & 0 \\ 0 & 0 & 1 & 0 \end{bmatrix}.$$

The internal leakage fault is considered in the following formula.

$$f_a(x_1, x_3, t) = -\frac{C_t \beta_e A}{J}\left(\frac{1}{V_1} + \frac{1}{V_2}\right)\sqrt{|P_L|}\text{sgn}(P_L) \qquad (9)$$

Assumption 1:

a) Except for the position sensor fault, all states are measured and bounded.

b) The sensor fault only occurs at the displacement sensor and the remaining sensors are healthy.

c) The position sensor fault and internal leakage fault change gradually.

d) $f_a(x_1, x_3, t)$ and its derivative are bounded signal, i.e., $f_{amin} \leq f_a \leq f_{amax}$.

Notations: Given vector $\mathbf{c} \in R^n$ and matrix $\mathbf{D} \in R^{m \times n}$, $\|\mathbf{c}\|^2 = c^T c$ and $\|\mathbf{D}\|^2 = \mathrm{tr}\left(D^T D\right)$

Remark 1: The ideal of the control objective is to guarantee a great position tracking performance under external disturbance, model uncertainty, actuator fault, and position sensor fault. Inspired by the position sensor fault detection, the FDI and the FTC are designed to achieve the control objective for the plant (8).

Remark 2: The faulty condition occurs not only a single fault, i.e., actuator fault or position sensor fault but also a simultaneous defective situation.
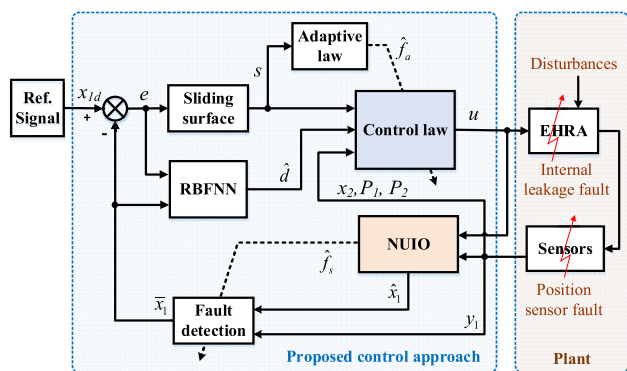

FIGURE 2. Block diagram of the proposed control scheme.

III. FAULT DETECTION AND CONTROLLER DESIGN FOR EHRA

The proposed control approach is described in Fig. 2, which includes two main modules. At the firstly key block, the FDI module based on NUIO is designed to detect and identify fault occurring at the position sensor. Since the position sensor fault is detected, the estimated position replaces the measured position. Meantime, either the estimated position or the measured position is feedbacked to the controller relying on the FD result. Then, the FTC module using ABTSMC with RBFNN approximator is employed to alleviate the effects of the mismatched disturbance. Additionally, the projection adaptive law is proposed to handle the internal leakage fault. During the simultaneously concerned faults occurring in the system, the proposed controller ensures high accuracy tracking performance with a similar quality of the control system under healthy conditions.

A. NONLINEAR UNKNOWN INPUT OBSERVER

As above-mentioned, an observer is designed to estimate the sensor fault, while minimizing the effects of the internal leakage fault and mismatched disturbance/uncertainty. Taking advantage of the NUIO [34], [52], [53], the influences of the internal leakage fault and mismatched disturbance/uncertainty can be limited by considering them as unknown input components. Besides, based on the sensor

fault estimation, a fault detection mechanism is derived to make the decision.

To be more convenient for designing the NUIO, the total system model is rewritten as follows:

$$\dot{x} = \xi(x, u) + F\psi \tag{10}$$
$$y = Cx \tag{11}$$

where $F \in R^{4 \times 3}$ is a known disturbance matrix with an appropriate dimension, $\psi = [d, f_a, \zeta]^T$ is an unknown input vector, and $\xi(x, u) = [x_2, x_3 + h(x), f(x) + g(x)u, -k_s x_4]^T$.

Assumption 2: The nonlinear vector function $\xi(x, u)$ is assumed to satisfy the Lipschitz condition [32] as follows:

$$\left\| \xi(x, u) - \xi(\hat{x}, u) \right\| \leq \kappa \left\| x - \hat{x} \right\| \tag{12}$$

where κ is a Lipschitz constant and $\hat{x}$ is the estimation of x.

In order to simplify the notations in the following, let ξ, $\hat{\xi}$ denote $\xi(x, u)$, $\xi(\hat{x}, u)$, respectively. A nonlinear observer is designed for the new system (10), (11) in the form [18]:

$$\dot{z} = M\hat{\xi} + L\left(y - \hat{y}\right) \tag{13}$$
$$\hat{x} = z + Ny \tag{14}$$

where the unknown matrices N and L are designed to decouple the effect of unknown inputs from the state estimation error. The matrix M is defined as

$$M = I - NC \tag{15}$$

The state estimation error is defined as $\tilde{x} = x - \hat{x}$. From (10), (11), (13), and (14), its derivative is calculated by

$$\dot{\tilde{x}} = M\left(\xi - \hat{\xi}\right) + MF\psi - LC\left(x - \hat{x}\right) \tag{16}$$

To eliminate the effect of the unknown input component ψ, the following condition needs to be satisfied

$$MF = 0 \Leftrightarrow (I - NC)F = 0 \tag{17}$$

To obtain (17), the necessary and sufficient conditions are expressed as the following.

$$\mathrm{rank}(CF) = \mathrm{rank}(F) \tag{18}$$

Then, the general solution (17) is described as

$$N = N_1 + J_N N_2 \tag{19}$$

where

$$N_1 = F(CF)^+$$
$$N_2 = I - (CF)(CF)^+$$
$$(CF)^+ = [(CF)^T(CF)]^{-1}(CF)^T \tag{20}$$

and J_N is an arbitrary matrix.

Theorem 1: Applying the proposed observer (13), (14) to the plant (10), (11), the state estimation error asymptotically converges to zero, if there exists a positive symmetric matrix Q and two matrices F, L such that condition (17) and the following condition hold:

$$-Q(LC) - (LC)^T Q + \kappa QMM^T Q + \kappa I < 0 \tag{21}$$

Proof: See Appendix A.

Remark 3: The LMI (21) can be solved via MATLAB LMI control toolbox. Following (15) and (20), the procedure to obtain the NUIO is derived as follows:

1) Calculate N_1, N_2 from (20).

2) Obtain the matrices Q, J_N, and L by solving the following LMI:

$$\begin{bmatrix} \begin{pmatrix} -Q(LC) - (LC)^T Q \\ +\kappa I \end{pmatrix} & \sqrt{\kappa} \begin{pmatrix} Q(I - N_1 C) \\ -QJ_N N_2 C \end{pmatrix} \\ \sqrt{\kappa} \begin{pmatrix} Q(I - N_1 C) \\ -QJ_N N_2 C \end{pmatrix}^T & -I \end{bmatrix} < 0 \tag{22}$$

3. According to (15) and (19), the observer gains N, M are computed.

Remark 4: Either the estimation value of the NUIO or the measured signal is utilized in the total control system design. The FD mechanism is proposed by comparing the estimated position sensor fault with a threshold, which is determined as follows:

$$\bar{x}_1 = \begin{cases} y_1 & \text{if } |f_s| < \chi \\ \hat{x}_1 & \text{otherwise} \end{cases} \tag{23}$$

where $\hat{x}_1$ is the estimation value of x_1 based on the NUIO, χ is a threshold value that is selected to keep away from the false alarms caused by disturbances, uncertain parameters [35], [36], [48].

B. ADAPTIVE BACKSTEPPING TERMINAL SLIDING MODE CONTROLLER WITH RBF APPROXIMATOR

In this sub-section, the controller is constructed based on the backstepping terminal sliding mode technique to achieve not only high-tracking accuracy performance but also system stability in the presence of sensor and actuator faults. The proposed scheme retains the merits of the terminal sliding mode control including rapid response, robust high-precision control, and fast convergence. Furthermore, the advantage of the backstepping control technique in terms of globally asymptotic stability is based on the Lyapunov theory [46], [54], [55]. To handle the internal leakage fault as well as the mismatched disturbance, the RBFNN and the projection adaptive law are adopted, respectively. Finally, the final control law is synthesized to ensure the robustness with faults while maintaining the stability of the system.

To facilitate the recursive backstepping technique, the errors between the measurement value and the virtual signals are defined

$$z_i = x_i - x_{id}, \quad (i =, \overline{1, 3}) \tag{24}$$

where x_{1d} is the output trajectory, x_{2d} and x_{3d} are the virtual control laws for x_2 and x_3, respectively.

Considering the 1st equation of the total system (8), taking the derivative of z_1, one obtains

$$\dot{z}_1 = x_2 - \dot{x}_{1d} \tag{25}$$

In order to stabilize the system (25), a virtual control law is designed as

$$\begin{aligned} x_{2d} &= -k_1 \bar{z}_1 + \dot{x}_{1d} \\ &= -k_1 z_1 + \dot{x}_{1d} + k_1 \tilde{x}_1^* \end{aligned} \tag{26}$$

where $\bar{z}_1 = \bar{x}_1 - x_{1d}, \tilde{x}_1^* = x_1 - \bar{x}_1, k_1$ is a positive constant.

Substituting (26) into (25), then taking the derivative of z_1 with respect time, which becomes

$$\dot{z}_1 = -k_1 z_1 + k_1 \tilde{x}_1^* + z_2 \tag{27}$$

Meanwhile, the time derivative of z_2 can be obtained as

$$\dot{z}_2 = x_3 + h(x_2) + d(t, x_1, x_2) - \dot{x}_{2d} \tag{28}$$

To ensure the error z_2 to be as small as possible, the virtual control of x_3 is given by:

$$x_{3d} = -h(x_2) - k_2 z_2 - \hat{d} + \dot{x}_{2d} \tag{29}$$

where k_2 is a positive constant, $\hat{d}$ is the approximated value of the real term d based on an RBFNN which is described as follows:

$$\begin{aligned} d &= W_1^T \phi_1 + \varepsilon_1 \\ \hat{d} &= \hat{W}_1^T \phi_1 \end{aligned} \tag{30}$$

where $W_1, \hat{W}_1, \phi_1, \varepsilon_1$ are ideal neural network weight values, its estimated value, Gaussian function, and the approximation error, respectively. The basis function $\phi_1(x_{in})$ is commonly chosen to be Gaussian RBFs as

$$\phi_1(x_{in}) = \exp\left(-\frac{\|x_{in} - c_j\|^2}{2r_j^2}\right) \tag{31}$$

where $j = \overline{1, N}$, N is the number of the basis functions, $c_j = [c_{1j}\ c_{2j}]^T$ and r_j are the center and width of the Gaussian function, respectively. $x_{in} = [\bar{x}_1, x_2]$ is an input vector of NN.

Assumption 3: The approximation error and weight value are bounded as $\varepsilon_1 < \varepsilon_N, \|W\|_F < W_M$ where ε_N and W_M are positive constants.

The weight estimation error of the NN is defined as

$$\tilde{W}_1^T = W_1^T - \hat{W}_1^T \tag{32}$$

and the adaptive laws for weighing factors of the NN is designed by

$$\dot{\hat{W}}_1 = \Gamma_1(\phi_1 z_2 - \lambda_1 \hat{W}_1) \tag{33}$$

where Γ_1, λ_1 are positive constants.

Substituting (29) and (32) into (28), the derivative of z_2 is rewritten as follows:

$$\dot{z}_2 = -k_2 z_2 + \varepsilon_1 + \tilde{W}_1^T \phi_1 + z_3 \tag{34}$$

The terminal sliding surface is chosen as:

$$s = z_3 + \Lambda z_2^\alpha \tag{35}$$

where Λ is a positive definite; $\alpha = \alpha_1/\alpha_2, 1 > \alpha > 1/2, \alpha_1, \alpha_2$ are positive odd integers.

The dynamic of the sliding variable s is expressed as

$$\dot{s} = \dot{z}_3 + \Lambda \alpha z_2^{\alpha-1} \dot{z}_2 = f(x_1, x_2, x_3) + g(x_1)u$$
$$+ f_a(x_1, x_3, t) - \dot{x}_{3d} + \Lambda \alpha z_2^{\alpha-1} \dot{z}_2 \quad (36)$$

The duty of the final law control is to reduce the effect caused by fault while ensuring the system stability and acceptable accuracy tracking performance.

To implement the final law control, a fast TSM-type reaching phase [56] is designed as:

$$\dot{s} + \rho s + \lambda |s|^{\nu} sign(s) = 0 \quad (37)$$

where ρ, λ are two positive constants for the reaching phase, and $0 < \nu < 1$.

Hence, the control signal is designed as $u = u_a + u_r$ where u_a is a model compensation term and u_r is a robust term. The designs of these control signals are mentioned as follows:

$$u_a = \frac{1}{g(x_1)} \left(-f(\bar{x}_1, x_2, x_3) - \hat{f}_a + \dot{x}_{3d} - \Lambda \alpha z_2^{\alpha-1} \dot{z}_2 \right)$$
$$u_r = \frac{1}{g(x_1)} \left(-\rho s - \lambda |s|^{\nu} sgn(s) \right) \quad (38)$$

The adaptive law for the internal leakage fault is designed as

$$\dot{\hat{f}}_a = \text{Proj}_{\hat{f}_a} (\Gamma_2 s) \quad (39)$$

where the well-known projection mapping technique is utilized as

$$\text{Proj}_{\hat{f}_a} (\bullet) = \begin{cases} 0, & \text{if } \hat{f}_a = f_{a\,max} \text{ and } \bullet > 0 \\ 0, & \text{if } \hat{f}_a = f_{a\,min} \text{ and } \bullet < 0 \\ \bullet, & \text{otherwise} \end{cases} \quad (40)$$

and Γ_2 are positive constant.

In the design of u_a, the position signal $\bar{x}_1$ is utilized instead of x_1 and $\hat{f}_a$ is an estimation value of f_a. Hence, the approximated errors are determined as

$$\tilde{f} = f(x_1, x_2, x_3) - f(\bar{x}_1, x_2, x_3)$$
$$\tilde{f}_a = f_a - \hat{f}_a \quad (41)$$

From (38), (41), the time derivative of the sliding surface s can be expressed as:

$$\dot{s} = -\rho s - \lambda |s|^{\nu} + \tilde{f} + \tilde{f}_a \quad (42)$$

Remark 5: The singular problem can be avoided by using the modified terminal sliding surface as [57]

$$s = z_3 + \sigma(z_2) \quad (43)$$

where

$$\sigma(z_2) = \begin{cases} \Lambda z_2^{\alpha} & \text{if } \bar{s} = 0 \text{ or } \bar{s} \neq 0 \\ & \text{and } |z_2| > \Lambda_s \quad (44) \\ k_{1s}z_2 + k_{2s}z_2^2 sign(z_2) & \text{if } \bar{s} \neq 0 \text{ and } |z_2| \leq \Lambda_s \end{cases}$$

where $k_{1s} = (2-\nu)\Lambda_s^{\nu-1}$, $k_{2s} = (\nu-1)\Lambda_s^{\nu-2}$, Λ_s is a positive constant, and $\bar{s} = z_3 + \Lambda z_2^{\alpha}$.

Theorem 2: For the system (8), with the NUIO in (13), (14), if the control input signal is proposed as (38) with its parameter estimation law addressed as (33) and (39), that does not only guarantee the stability of the closed-loop control but also maintain good tracking control under faulty conditions.

Proof: See Appendix B.

Remark 6: The stability analysis in (50) is considered under a detected fault. In the circumstances, the magnitude of fault is smaller than the threshold, one obtains $\tilde{x}_1^* = x_1 - y_1$, $|f_s| \leq \chi$. The stability analysis can be easily completed by a similar approach. Hence, bounded tracking performance is achieved.

IV. NUMERICAL SIMULATION AND DISCUSSION
A. SIMULATION SETUP
To verify the effect of the proposed approach, numerical simulation is conducted in MATLAB Simulink environment as the sample time of 0.0001 seconds. The EHRA has been widely utilized as a benchmark EHA in research [2], [4]. Its parameters are described in Table 1. A reference trajectory is chosen in a sinusoidal-signal form as $q_d = 10\sin(t)$ (deg). The mismatched disturbance and the internal leakage fault are designed later based on the case study in the simulation results part. The position sensor fault happens at $t = 4s$ with $k_s = 1$, $\zeta = 10 + \sin(\pi t)$ (deg).

TABLE 1. Parameters of the EHRA system.

Symbol	Quantity	Value
J	Moment of inertia	0.37 kg.m^2
A	Radian displacement	1.2x10^{-4} m^3/rad
B	Viscous friction coefficient	45 N.m.s/rad
P_s	Supply pressure	10 MPa
P_r	Return pressure	0.1 MPa
β_e	Bulk modulus	1.5x10^3 MPa
k_t	Proportional gain	2x10^{-8} m^3/s/V/Pa$^{-1/2}$
C_0	Normal leakage coefficient	1.8x10^{-12} m^5/Ns
C_{t0}	Leakage fault coefficient	4.5x10^{-10} m^4/(N$^{1/2}$s)
α	The rate of fault evolution	10

Four controllers are carried out to test on the EHRA in this work. Their results are compared to demonstrate the effectiveness of the suggested methodology. Firstly, based on the trial-error procedure, the control gains of the proposed controller (ABTSMC) are set as $k_1 = 15$, $k_2 = 50$, $\lambda_1 = 0.1$, $\Gamma_1 = 500$, $\Gamma_2 = 1500$, $\Lambda = 6$, $\alpha_1 = 7$, $\alpha_2 = 9$, $\nu = 5/7$, $\lambda = 50$, $\rho = 50$. The structure of the NN consists of three layers and the parameters of Gaussian function RBF-NN in the hidden layers are chosen according to cover the feasible working range of each input. Consider the range of the first input and second input are $[-30; 30]$ (deg) and $[-30; 30]$ (deg/s), respectively. c_i, r_i are designed as $c_i = [-30 \ -20 \ -10 \ 0 \ 10 \ 20 \ 30; -30 \ -20 \ -10 \ 0 \ 10 \ 20 \ 30]$, $r_i = 15$. The initial weight value is chosen as zeros. The parameters of the NUIO, which are obtained by solving the LMI via MATLAB

LMI control toolbox, are given as

$$Q = \begin{bmatrix} 17.0351 & 0 & 0 & 17.0876 \\ 0 & 34.1227 & 0 & 0 \\ 0 & 0 & 34.1227 & 0 \\ 17.0876 & 0 & 0 & 17.0351 \end{bmatrix}$$

$$J_N = \begin{bmatrix} 0 & 0 & 0 \\ 0 & 1 & 0 \\ 0 & 0 & 1 \\ 0 & 0 & 0 \end{bmatrix}, \quad L = \begin{bmatrix} 0.2793 & 0 & 0 \\ 0 & 0.5586 & 0 \\ 0 & 0 & 0.5586 \\ 0.2793 & 0 & 0 \end{bmatrix}$$

The position threshold value is carefully selected and set to $\chi = 5°$.

The second controller is a backstepping terminal sliding mode controller (TSMC) which does not consist of the RBFNN approximator and the projection adaptive law. To ensure a fair comparison, the parameters of the TSMC with compensations of NUIO are suitably selected similar to the proposed controller. The NUIO is utilized here with the same parameters as the proposed controller.

Next, the control gains of the proportional-integral-derivative (PID) control with sensor fault compensation (PIDC) are selected as $k_p = 50$, $k_i = 10$, $k_d = 1.3$. Because of the well-known technique, the design of PID is skipped in this paper and can be searched in [9], [12]. Finally, the PID controller without NUIO is applied under the same parameter as the PIDC.

In order to verify the effectiveness of the proposed control when the fault occurs, the following case studies are

derived

1. Only position sensor fault.

2. Simultaneous position sensor fault and mismatched disturbance.

3. Simultaneous position sensor fault, internal leakage fault, and mismatched disturbance.

B. SIMULATION RESULT

The NUIO is of importance in the control design. Especially, the position sensor fault is considered together with internal leakage fault and mismatched disturbance. Hence, first of all, the estimation performance of the NUIO is verified. A simple simulation is conducted, and the results are illustrated in Fig. 3. As seen, the NUIO successfully estimates the position sensor fault (Fig. 3a) as well as the true angular displacement (Fig. 3c) in the presence of the additive sensor fault, internal leakage fault, and mismatched disturbance. Moreover, the flag switch of the fault detection is immediately changed (Fig. 3b) when the sensor fault estimation is bigger than the threshold at the time $t = 4.5s$. It is worth noting that fault occurs at the time $t = 4s$ but the fault is detected at the time $t = 4.5s$ because of the dependence on the threshold value.

1) CASE STUDY 1

In this case study, we assume that the fault only occurs in the position sensor. The response results of the comparative controllers, in turn, the tracking position, the error state, and the control input are described in Fig. 4. It is observed that the
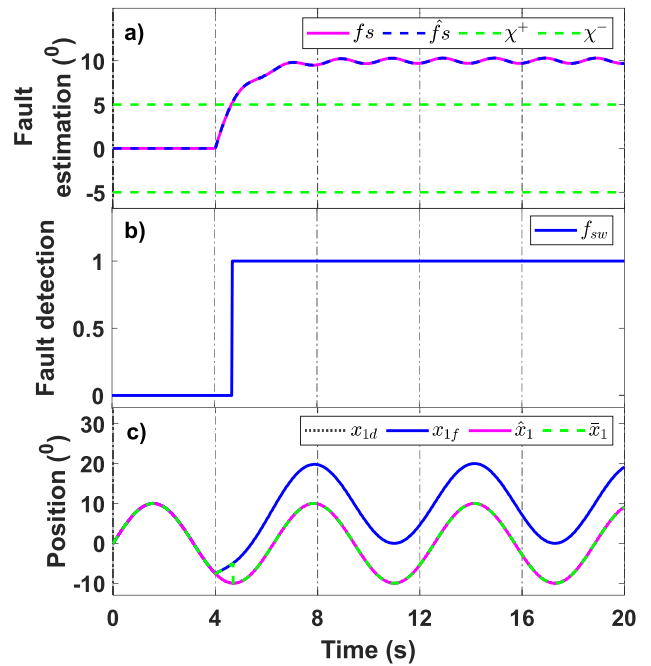

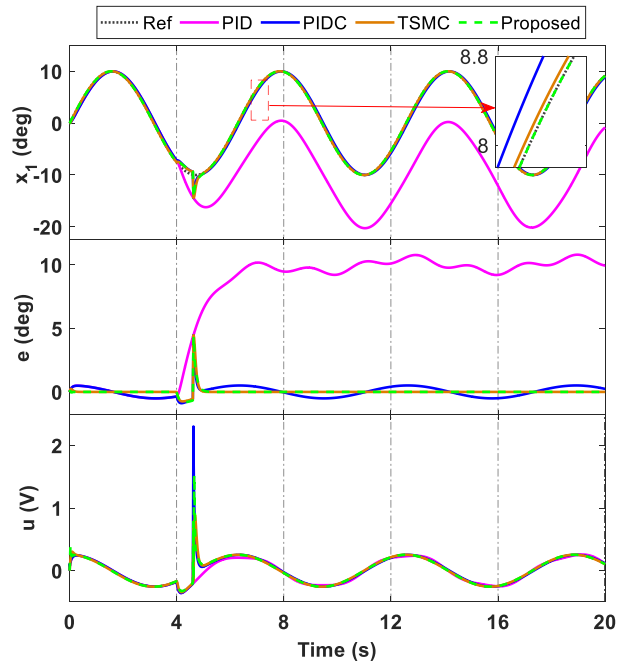**FIGURE 3.** Fault estimation, fault flag and position.

FIGURE 4. Performances of the comparative controllers in case study 1.

fault is detected after 4.5s, the proposed FTC is reconfigured, i.e., the measured position instead of the estimated position. So, the tracking performances of the proposed controller, TSMC and PIDC are impacted when the switching action happens. However, the displacement of the rotary actuator gradually recovers and tracks its reference trajectory without any serious influence of the fault. In order to compare the recovery of these FTC as well as tracking performance, the performance index, namely, the integral absolute error (IAE)
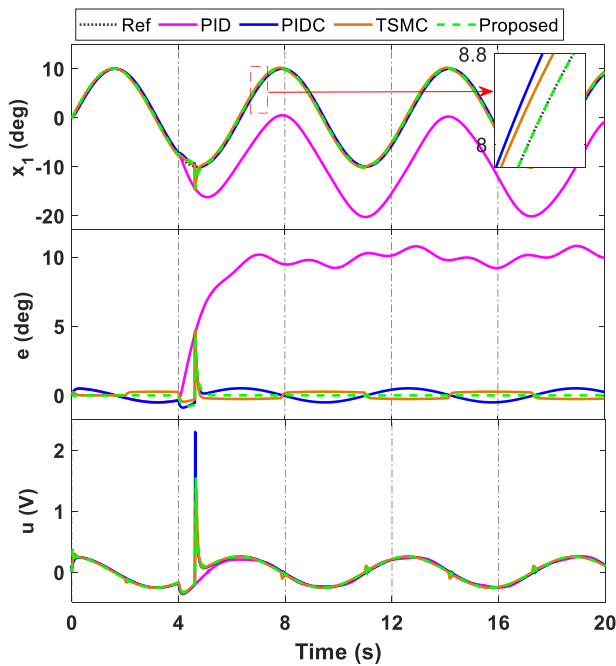
FIGURE 5. Performances of the comparative controllers in case study 2.

FIGURE 6. Performances of the comparative controller in case study 3.

$(L_2[e] = \sqrt{\left(\int_0^T |e|^2 dt\right)/T})$ (deg) are approximately given as 8.56°, 0.43°, 0.28°, and 0.24° for PID, PIDC, TSMC, and proposed controller, respectively. Among these controllers, the performance of the PID controller is the worse with severe tracking error when the fault occurs because the sensor fault compensation is not included here. In contrast, thanks to the support of the NUIO, high accuracy tracking performances are realized in the remained controllers, especially the proposed controller due to the robustness of ABTSMC. In addition, control signals of three controllers are presented at the same level, without any large difference except for the PIDC with a pulse when the fault is detected.

2) CASE STUDY 2
Besides the position sensor fault, the mismatched disturbance is added in this case study to validate the robustness of the proposed controller compared to the remains. In the practical hydraulic system, it is difficult to achieve the precise mathematical model of the mismatched disturbances. So, for the sake of results' evaluation, it is hypothetical and can be designed in the following form:

$$d_1 = \begin{cases} 0 & \text{if } t \le 2s \\ 5x_2 + 1.5\text{sign}(x_2) & \text{otherwise} \end{cases} \tag{45}$$

The simulation results are presented in Fig. 5 under a similar situation with case study 1. In the presence of the mismatched disturbance, the IAEs of the PID, PIDC, TSMC, and proposed controller, in turn, 8.6°, 0.46°, 0.32°, and 0.24°. It is clear that the tracking performance of the proposed controller is much better than the TSMC and PIDC by employing the NN approximator to take care of the mismatched disturbance.
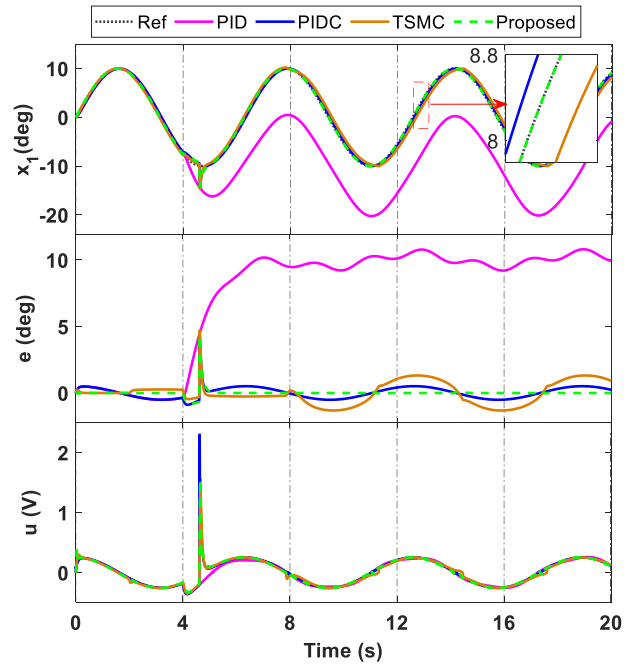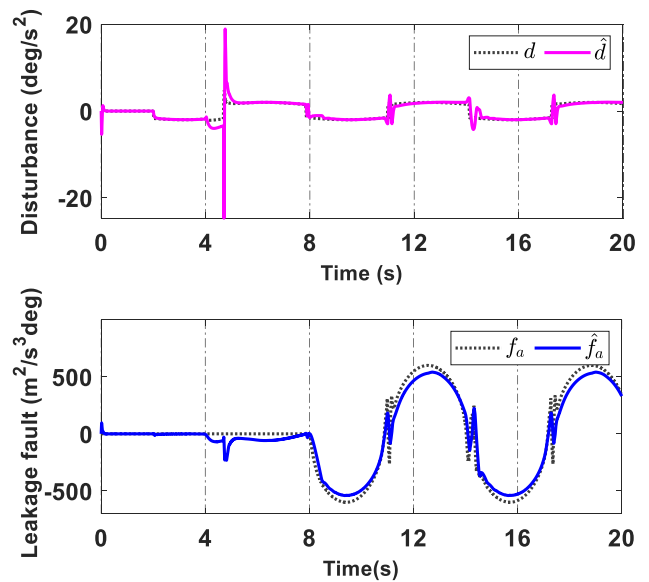

FIGURE 7. Mismatched disturbance and internal leakage fault estimation performance.

3) CASE STUDY 3
In the third study, the internal leakage is simultaneously considered together with the position sensor fault and mismatched disturbance to test the performances of comparative controllers. To simulate the internal leakage fault, the following slow-varying faulty coefficient is selected as

$$C_t = \begin{cases} 0 & \text{if } t < 8s \\ (1 - e^{-\alpha(t-8)})C_{t0} & \text{otherwise} \end{cases} \tag{46}$$

It means that the abrupt internal leakage fault occurs from the time $t \ge 8s$. Fig. 6 shows that even under severe

conditions, the NUIO still completes its role to detect and estimate the position sensor fault, which is compensated in the control design of the proposed controller, TSMC and PIDC. Due to the effect of both internal leakage fault and mismatched disturbance, the IAE are 8.8°, 0.49°, 0.82°, and 0.25° for PID, PIDC, TSMC and proposed controller, respectively. However, the projection update law adapts the internal leakage fault and the NN approximation helps to tackle the mismatched disturbance. Thus, the proposed controller achieves the best tracking performance.

The estimation performance of the mismatched disturbance and the internal leakage fault are depicted in Fig. 7a and Fig. 7b, respectively. The estimated values successfully track its physical values, which make contributions to the final position tracking performance of the proposed controller shown in Fig. 6.

From the simulation results, it can be concluded that the proposed fault-tolerant controller shows the high-accuracy position tracking performance under a bunch of problems including position sensor fault, mismatched disturbance, and internal leakage fault.

V. CONCLUSION

This paper has developed a new active FTC to deal with the simultaneous sensor fault and actuator fault in the EHRA system based on the combination of a novel observer and adaptive control laws. In detail, the novel NUIO technique is proposed to estimate both the sensor fault and the rotary angular displacement, whilst the integration of the RBFNN and the projection adaptive law into the adaptive backstepping terminal sliding mode control is adopted to handle the internal leakage fault and mismatched disturbance. Thus, the proposed controller can guarantee control performance when the sensor fault, internal leakage fault, and mismatched disturbance exist in the system. The stability of the control system is analyzed based on the Lyapunov theory. The effectiveness of the proposed controller has been verified by the numerical simulation results. Future research will be conducted to improve the control design and test the algorithm on a real test bench.

APPENDIX A

The Lyapunov function is selected in the form

$$V_0 = \tilde{x}^T Q \tilde{x} \qquad (47)$$

Differentiating both sides of (47) and utilizing Assumption 2, (16) and condition (17), one obtains

$$\dot{V}_0 = -\tilde{x}^T (QLC + (LC)^T Q)\tilde{x} + 2\tilde{x}^T QM \left(\xi - \hat{\xi} \right)$$
$$\leq -\tilde{x}^T \left(QLC + (LC)^T Q \right) \tilde{x} + 2\kappa \|\tilde{x}QM\| \|\tilde{x}\|$$
$$\leq -\tilde{x}^T \left(QLC + (LC)^T Q \right) \tilde{x} + \kappa \left(\|\tilde{x}QM\|^2 + \|\tilde{x}\|^2 \right)$$
$$= -\tilde{x}^T \left(QLC + (LC)^T Q - \kappa QMM^T Q - \kappa I \right) \tilde{x}$$
$$= -\tilde{x}^T P \tilde{x} \qquad (48)$$

where $P = QLC + (LC)^T Q - \kappa QMM^T Q - \kappa I$. If (21) is satisfied, from (48), it is concluded that the state estimation errors asymptotically converge to zeros in a certain time. The proof is completed.

APPENDIX B

The Lyapunov function is considered as

$$V = \tilde{x}^T Q \tilde{x} + \frac{1}{2} z_1^2 + \frac{1}{2} z_2^2 + \frac{1}{2} s^2$$
$$+ \frac{1}{2} \tilde{W}_1^T \Gamma_1^{-1} \tilde{W}_1 + \frac{1}{2} \Gamma_2^{-1} \tilde{f}_a^2 \qquad (49)$$

Taking derivative is calculated along (48), (27), (34), sliding surface (42), the adaptive laws (33) and (39), after the position sensor fault is detected (i.e. $\tilde{x}_1^* = \tilde{x}_1$), one obtains

$$\dot{V} = -\tilde{x}^T P \tilde{x} - k_1 z_1^2 - k_2 z_2^2 - \rho s^2 - \lambda |s|^{\nu+1} + k_1 \tilde{x}_1^* z_1$$
$$+ z_1 z_2 + z_2 s - \Lambda z_2^{\alpha+1} - \tilde{W}_1^T \Gamma_1^{-1} (\dot{\hat{W}}_1 - \Gamma_1 \phi_1 z_2)$$
$$- \Gamma_2^{-1} \tilde{f}_a (\dot{\hat{f}}_a - \Gamma_2 s) + s \tilde{f} + z_2 \varepsilon_1 + \Gamma_2^{-1} \tilde{f}_a \dot{f}_a$$
$$\leq -\tilde{x}^T P \tilde{x} - k_1 z_1^2 - k_2 z_2^2 - \rho s^2 - \lambda |s|^{\nu+1} + k_1 \tilde{x}_1 z_1$$
$$+ z_1 z_2 + z_2 s - \Lambda z_2^{\alpha+1} + \lambda_1 \tilde{W}_1^T \left(W_1 - \tilde{W}_1 \right)$$
$$+ s \tilde{f} + z_2 \varepsilon_1 + \Gamma_2^{-1} \tilde{f}_a \dot{f}_a \qquad (50)$$

Using Young's inequality, the following inequality holds

$$\dot{V} \leq -\tilde{x}^T \text{diag} \left(\lambda_p - \frac{k_1}{2}, \lambda_p, \lambda_p, \lambda_p \right) \tilde{x} - \frac{1}{2} (k_1 - 1) z_1^2$$
$$- \left(k_2 - \frac{3}{2} \right) z_2^2 - (\rho - 1)s^2 - \frac{1}{2} \lambda_1 \tilde{W}_1^T \tilde{W}_1$$
$$+ \frac{1}{2} \lambda_1 W_1^T W_1 + \frac{1}{2} \tilde{f}^2 + \frac{1}{2} \varepsilon_1^2 + \frac{1}{2} \Gamma_2^{-1} \left(\tilde{f}_a^2 + \dot{f}_a^2 \right)$$
$$\leq -\Psi + \delta \qquad (51)$$

where $\lambda_P = \lambda_{\min}(P)$ is a minimum eigenvalue of matrix P,

$$\Psi = \tilde{x}^T \text{diag} \left(\lambda_p - \frac{k_1}{2}, \lambda_p, \lambda_p, \lambda_p \right) \tilde{x} + \frac{1}{2} (k_1 - 1) z_1^2$$
$$+ \left(k_2 - \frac{3}{2} \right) z_2^2 + (\rho - 1)s^2 + \frac{1}{2} \lambda_1 \tilde{W}_1^T \tilde{W}_1,$$

$$\delta = \sup \left\{ \frac{1}{2} \lambda_1 W_1^T W_1 + \frac{1}{2} \tilde{f}^2 + \frac{1}{2} \varepsilon_1^2 + \frac{1}{2} \Gamma_2^{-1} \left(\tilde{f}_a^2 + \dot{f}_a^2 \right) \right\}.$$

From the extended version of Barbalat's Lemma in Appendix C, it is easy to state that when $t \to \infty$, $\Psi \to \Psi_\infty \leq \delta$. Hence, bounded tracking performance is achieved. In our future work, the asymptotic tracking control will be developed to further improve the superiority of the proposed method [58].

APPENDIX C

Extended Barbalat's Lemma: For a non-autonomous system $\dot{x} = f(x, t)$. If there exist positive-definite functions $V, W \geq 0$ satisfying $\dot{V} \leq -W + \Delta$ where Δ is a positive constant, $\ddot{V}$ is bounded, and W is continuous, one of the following situations occur

    1) $t \to \infty \Rightarrow W \to \Delta$

2) $t \to \infty \Rightarrow W < \Delta$

Proof:

Define $\Omega_0 = \{x|W \geq \Delta\}$, $\Omega_1 = \{x|W < \Delta\}$. If $x(t_0) \in \Omega_0$, the following 2 situations are considered:

1) If $x(t) \in \Omega_0 \; \forall t > t_0$, Barbalat's Lemma [59] is directly applied here to conclude that $W \to \Delta$ when $t \to \infty$.

2) If $\exists t_1 > 0 : \; x(t_1) \in \Omega_1$, then the following cases are considered:

   a) If $x(t) \in \Omega_1 \; \forall t > t_1$, one obtains $W(x(t)) < \Delta \; \forall t > t_1$.

   b) If $\exists t_2 > t_1 : \; x(t_2) \in \Omega_0$. Because W is continuous, it is possible to choose t_2 to obtain $0 < W - \Delta < \varepsilon$, $\forall \varepsilon > 0$. The situation is the same as when $t = t_0$. Then, the arguments are repeated.

Hence, the proof of the extended Barbalat's Lemma is completed.

REFERENCES

[1] J. Yao, "Model-based nonlinear control of hydraulic servo systems: Challenges, developments and perspectives," *Frontiers Mech. Eng.*, vol. 13, no. 2, pp. 179–210, Jun. 2018.

[2] J. Yao, Z. Jiao, D. Ma, and L. Yan, "High-accuracy tracking control of hydraulic rotary actuators with modeling uncertainties," *IEEE/ASME Trans. Mechatronics*, vol. 19, no. 2, pp. 633–641, Apr. 2014.

[3] Q.-N. Xu, K.-M. Lee, H. Zhou, and H.-Y. Yang, "Model-based fault detection and isolation scheme for a rudder servo system," *IEEE Trans. Ind. Electron.*, vol. 62, no. 4, pp. 2384–2396, Apr. 2015.

[4] J. Yao, G. Yang, and Z. Jiao, "High dynamic feedback linearization control of hydraulic actuators with backstepping," *Proc. Inst. Mech. Eng., I, J. Syst. Control Eng.*, vol. 229, no. 8, pp. 728–737, Sep. 2015.

[5] J. Yao, Z. Jiao, and D. Ma, "Extended-state-observer-based output feedback nonlinear robust control of hydraulic systems with backstepping," *IEEE Trans. Ind. Electron.*, vol. 61, no. 11, pp. 6285–6293, Nov. 2014.

[6] D.-T. Tran, T.-C. Do, and K.-K. Ahn, "Extended high gain observer-based sliding mode control for an electro-hydraulic system with a variant payload," *Int. J. Precis. Eng. Manuf.*, vol. 20, no. 12, pp. 2089–2100, Dec. 2019.

[7] Z. Yao, J. Yao, and W. Sun, "Adaptive RISE control of hydraulic systems with multilayer neural-networks," *IEEE Trans. Ind. Electron.*, vol. 66, no. 11, pp. 8638–8647, Nov. 2019.

[8] O. Doukhi and D. J. Lee, "Neural network-based robust adaptive certainty equivalent controller for quadrotor UAV with unknown disturbances," *Int. J. Control, Autom. Syst.*, vol. 17, no. 9, pp. 2365–2374, Sep. 2019.

[9] V. T. Yen, W. Y. Nan, and P. Van Cuong, "Robust adaptive sliding mode neural networks control for industrial robot manipulators," *Int. J. Control, Autom. Syst.*, vol. 17, no. 3, pp. 783–792, Mar. 2019.

[10] G. Tan, Z. Wang, and C. Li, "H∞ performance state estimation of delayed static neural networks based on an improved proportional-integral estimator," *Appl. Math. Comput.*, vol. 370, Apr. 2020, Art. no. 124908.

[11] L. Liu, Y.-J. Liu, D. Li, S. Tong, and Z. Wang, "Barrier Lyapunov function-based adaptive fuzzy FTC for switched systems and its applications to resistance–inductance–capacitance circuit system," *IEEE Trans. Cybern.*, vol. 50, no. 8, pp. 3491–3502, Aug. 2020.

[12] C. P. Vo, X. D. To, and K. K. Ahn, "A novel adaptive gain integral terminal sliding mode control scheme of a pneumatic artificial muscle system with time-delay estimation," *IEEE Access*, vol. 7, pp. 141133–141143, 2019.

[13] Y. Wang, X. Zhang, L. Yang, and H. Huang, "Adaptive synchronization of time delay chaotic systems with uncertain and unknown parameters via aperiodically intermittent control," *Int. J. Control, Autom. Syst.*, vol. 18, no. 3, pp. 696–707, Mar. 2020.

[14] X. Yu and J. Jiang, "A survey of fault-tolerant controllers based on safety-related issues," *Annu. Rev. Control*, vol. 39, pp. 46–57, Jan. 2015.

[15] I. Hwang, S. Kim, Y. Kim, and C. E. Seah, "A survey of fault detection, isolation, and reconfiguration methods," *IEEE Trans. Control Syst. Technol.*, vol. 18, no. 3, pp. 636–653, May 2010.

[16] S. A. Nahian, D. Q. Truong, P. Chowdhury, D. Das, and K. K. Ahn, "Modeling and fault tolerant control of an electro-hydraulic actuator," *Int. J. Precis. Eng. Manuf.*, vol. 17, no. 10, pp. 1285–1297, Oct. 2016.

[17] M. S. Shaker and R. J. Patton, "Active sensor fault tolerant output feedback tracking control for wind turbine systems via T–S model," *Eng. Appl. Artif. Intell.*, vol. 34, pp. 1–12, Sep. 2014.

[18] J. Zarei and J. Poshtan, "Design of nonlinear unknown input observer for process fault detection," *Ind. Eng. Chem. Res.*, vol. 49, no. 22, pp. 11443–11452, Nov. 2010.

[19] H. Chen, B. Jiang, and N. Lu, "A multi-mode incipient sensor fault detection and diagnosis method for electrical traction systems," *Int. J. Control, Autom. Syst.*, vol. 16, no. 4, pp. 1783–1793, Aug. 2018.

[20] S. K. Kommuri, S. B. Lee, and K. C. Veluvolu, "Robust sensors-fault-tolerance with sliding mode estimation and control for PMSM drives," *IEEE/ASME Trans. Mechatronics*, vol. 23, no. 1, pp. 17–28, Feb. 2018.

[21] Z. Wang, L. Liu, and H. Zhang, "Neural network-based model-free adaptive fault-tolerant control for discrete-time nonlinear systems with sensor fault," *IEEE Trans. Syst., Man, Cybern. Syst.*, vol. 47, no. 8, pp. 2351–2362, Aug. 2017.

[22] Z. Gao, C. Cecati, and S. Ding, "A survey of fault diagnosis and fault-tolerant techniques—Part II: Fault diagnosis with knowledge-based and hybrid/active approaches," *IEEE Trans. Ind. Electron.*, vol. 62, no. 6, pp. 3768–3774, Jun. 2015.

[23] Z. Gao, C. Cecati, and S. X. Ding, "A survey of fault diagnosis and fault-tolerant techniques—Part I: Fault diagnosis with model-based and signal-based approaches," *IEEE Trans. Ind. Electron.*, vol. 62, no. 6, pp. 3757–3767, Jun. 2015.

[24] P. Halder, "A novel approach for detection and diagnosis of process and sensor faults in electro-hydraulic actuator," *Int. J. Eng. Res. Develop.*, vol. 6, no. 7, pp. 15–22, 2013.

[25] H. Chen, B. Jiang, S. X. Ding, and B. Huang, "Data-driven fault diagnosis for traction systems in high-speed trains: A survey, challenges, and perspectives," *IEEE Trans. Intell. Transp. Syst.*, early access, Oct. 22, 2020, doi: 10.1109/TITS.2020.3029946.

[26] H.-J. Ma and G.-H. Yang, "Simultaneous fault diagnosis for robot manipulators with actuator and sensor faults," *Inf. Sci.*, vol. 366, pp. 12–30, Oct. 2016.

[27] S. Gayaka and B. Yao, "Fault detection, identification and accommodation for an electro-hydraulic system: An adaptive robust approach," in *Proc. 17th IFAC World Congr.*, 2008, pp. 13815–13820.

[28] C. P. Vo, X. D. To, and K. K. Ahn, "A novel force sensorless reflecting control for bilateral haptic teleoperation system," *IEEE Access*, vol. 8, pp. 96515–96527, 2020.

[29] S. Gautam, P. K. Tamboli, K. Roy, V. H. Patankar, and S. P. Duttagupta, "Sensors incipient fault detection and isolation of nuclear power plant using extended Kalman filter and Kullback–Leibler divergence," *ISA Trans.*, vol. 92, pp. 180–190, Sep. 2019.

[30] H. Liu, D. Liu, C. Lu, and X. Wang, "Fault diagnosis of hydraulic servo system using the unscented Kalman filter," *Asian J. Control*, vol. 16, no. 6, pp. 1713–1725, Nov. 2014.

[31] D. S. Pires and G. L. D. O. Serra, "Methodology for evolving fuzzy Kalman filter identification," *Int. J. Control, Autom. Syst.*, vol. 17, no. 3, pp. 793–800, Mar. 2019.

[32] S. Mondal, G. Chakraborty, and K. Bhattacharyy, "LMI approach to robust unknown input observer design for continuous systems with noise and uncertainties," *Int. J. Control, Autom. Syst.*, vol. 8, no. 2, pp. 210–219, Apr. 2010.

[33] T. Van Nguyen and C. Ha, "Experimental study of sensor fault-tolerant control for an electro-hydraulic actuator based on a robust nonlinear observer," *Energies*, vol. 12, no. 22, p. 4337, Nov. 2019.

[34] Z. Gao, X. Liu, and M. Chen, "Unknown input observer-based robust fault estimation for systems corrupted by partially decoupled disturbances," *IEEE Trans. Ind. Electron.*, vol. 63, no. 4, pp. 2537–2547, Apr. 2016.

[35] S. A. Nahian, T. Q. Dinh, H. V. Dao, and K. K. Ahn, "An unknown input observer–EFIR combined estimator for electrohydraulic actuator in sensor fault-tolerant control application," *IEEE/ASME Trans. Mechatronics*, vol. 25, no. 5, pp. 2208–2219, Oct. 2020.

[36] S. K. Kommuri, M. Defoort, H. R. Karimi, and K. C. Veluvolu, "A robust observer-based sensor fault-tolerant control for PMSM in electric vehicles," *IEEE Trans. Ind. Electron.*, vol. 63, no. 12, pp. 7671–7681, Dec. 2016.

[37] T. Li, T. Yang, Y. Cao, R. Xie, and X. Wang, "Disturbance-estimation based adaptive backstepping fault-tolerant synchronization control for a dual redundant hydraulic actuation system with internal leakage faults," *IEEE Access*, vol. 7, pp. 73106–73119, 2019.

[38] D. Wu, W. Liu, J. Song, and Y. Shen, "Fault estimation and fault-tolerant control of wind turbines using the SDW-LSI algorithm," *IEEE Access*, vol. 4, pp. 7223–7231, 2016.

[39] G. Ren, M. Esfandiari, J. Song, and N. Sepehri, "Position control of an electrohydrostatic actuator with tolerance to internal leakage," *IEEE Trans. Control Syst. Technol.*, vol. 24, no. 6, pp. 2224–2232, Nov. 2016.

[40] J. Yao, G. Yang, and D. Ma, "Internal leakage fault detection and tolerant control of single-rod hydraulic actuators," *Math. Problems Eng.*, vol. 2014, pp. 1–14, Mar. 2014.

[41] X. Wu, Y. Li, F. Li, Z. Yang, and W. Teng, "Adaptive estimation-based leakage detection for a wind turbine hydraulic pitching system," *IEEE/ASME Trans. Mechatronics*, vol. 17, no. 5, pp. 907–914, Oct. 2012.

[42] A. El-Betar, M. Abdelhamed, A. El-Assal, and R. Abdelsatar, "Fault diagnosis of a hydraulic power system using an artificial neural network," *J. King Abdulaziz Univ.-Eng. Sci.*, vol. 17, no. 1, pp. 115–136, 2006.

[43] A. Maddahi, W. Kinsner, and N. Sepehri, "Internal leakage detection in electrohydrostatic actuators using multiscale analysis of experimental data," *IEEE Trans. Instrum. Meas.*, vol. 65, no. 12, pp. 2734–2747, Dec. 2016.

[44] A. Y. Goharrizi and N. Sepehri, "A wavelet-based approach for external leakage detection and isolation from internal leakage in valve-controlled hydraulic actuators," *IEEE Trans. Ind. Electron.*, vol. 58, no. 9, pp. 4374–4384, Sep. 2011.

[45] A. Y. Goharrizi and N. Sepehri, "Internal leakage detection in hydraulic actuators using empirical mode decomposition and Hilbert spectrum," *IEEE Trans. Instrum. Meas.*, vol. 61, no. 2, pp. 368–378, Feb. 2012.

[46] M. Van, M. Mavrovouniotis, and S. S. Ge, "An adaptive backstepping nonsingular fast terminal sliding mode control for robust fault tolerant control of robot manipulators," *IEEE Trans. Syst., Man, Cybern. Syst.*, vol. 49, no. 7, pp. 1448–1458, Jul. 2019.

[47] A. T. Vo and H.-J. Kang, "A novel fault-tolerant control method for robot manipulators based on non-singular fast terminal sliding mode control and disturbance observer," *IEEE Access*, vol. 8, pp. 109388–109400, 2020.

[48] S. S.-D. Xu, C.-C. Chen, and Z.-L. Wu, "Study of nonsingular fast terminal sliding-mode fault-tolerant control," *IEEE Trans. Ind. Electron.*, vol. 62, no. 6, pp. 3906–3913, Jun. 2015.

[49] W. Liu, S.-Y. Chen, and H.-X. Huang, "Double closed-loop integral terminal sliding mode for a class of underactuated systems based on sliding mode observer," *Int. J. Control, Autom. Syst.*, vol. 18, no. 2, pp. 339–350, Feb. 2020.

[50] A. T. Vo and H.-J. Kang, "An adaptive terminal sliding mode control for robot manipulators with non-singular terminal sliding surface variables," *IEEE Access*, vol. 7, pp. 8701–8712, 2019.

[51] K. Eliker and W. Zhang, "Finite-time adaptive integral backstepping fast terminal sliding mode control application on quadrotor UAV," *Int. J. Control, Autom. Syst.*, vol. 18, no. 2, pp. 415–430, Feb. 2020.

[52] J. Chen, "Robust fault diagnosis of stochastic systems with unknown disturbances," in *Proc. Int. Conf. Control*, vol. 2, 1994, pp. 1340–1345.

[53] J. Li, Z. Wang, Y. Shen, and Y. Liu, "Unknown input observer design for Takagi–Sugeno systems with fuzzy output equation," *Int. J. Control, Autom. Syst.*, vol. 17, no. 1, pp. 267–272, Jan. 2019.

[54] L. Liu, Y.-J. Liu, A. Chen, S. Tong, and C. L. P. Chen, "Integral barrier Lyapunov function-based adaptive control for switched nonlinear systems," *Sci. China Inf. Sci.*, vol. 63, no. 3, pp. 1–14, Mar. 2020.

[55] D. T. Tran, D. X. Ba, and K. K. Ahn, "Adaptive backstepping sliding mode control for equilibrium position tracking of an electrohydraulic elastic manipulator," *IEEE Trans. Ind. Electron.*, vol. 67, no. 5, pp. 3860–3869, May 2020.

[56] T. X. Dinh, T. D. Thien, T. H. V. Anh, and K. K. Ahn, "Disturbance observer based finite time trajectory tracking control for a 3 DOF hydraulic manipulator including actuator dynamics," *IEEE Access*, vol. 6, pp. 36798–36809, 2018.

[57] L. Wang, T. Chai, and L. Zhai, "Neural-network-based terminal sliding-mode control of robotic manipulators including actuator dynamics," *IEEE Trans. Ind. Electron.*, vol. 56, no. 9, pp. 3296–3304, Sep. 2009.

[58] W. Deng and J. Yao, "Asymptotic tracking control of mechanical servosystems with mismatched uncertainties," *IEEE/ASME Trans. Mechatronics*, early access, Oct. 30, 2020, doi: 10.1109/TMECH.2020.3034923.

[59] H. K. Khalil, *Nonlinear Systems*. Upper Saddle River, NJ, USA: Prentice-Hall, 2002.
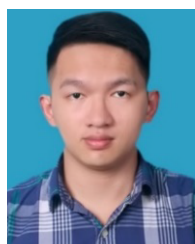
VAN DU PHAN received the B.S. degree in electrical engineering from the Hanoi University of Science and Technology, Hanoi, Vietnam, in 2013, and the M.Sc. degree in electrical engineering from the Thai Nguyen University of Technology, Thai Nguyen, Vietnam, in 2017. He is currently pursuing the Ph.D. degree with the School of Mechanical Engineering, University of Ulsan, Ulsan, South Korea.

His research interests include soft robot, hydraulic robot, nonlinear control, and fault tolerant control.

CONG PHAT VO received the B.E. degree in electrical and electronic engineering technology, in 2013, the M.Sc. degree in mechatronics engineering from the Ho Chi Minh City University of Technology and Education, Vietnam, in 2016, and the Ph.D. degree in mechanical and automotive engineering from the Department of Mechanical Engineering, University of Ulsan, Ulsan, South Korea, in 2021.

His research interests include intelligent control, soft robot, haptic control, and renewable energy.

HOANG VU DAO received the B.E. degree in mechatronics from the School of Mechanical Engineering, Hanoi University of Science and Technology, Vietnam, in 2018. He is currently pursuing the Ph.D. degree in mechanical engineering with the School of Mechanical Engineering, University of Ulsan, Ulsan, South Korea.

His current research interests include hydraulic robot, nonlinear control, and fault tolerant control.

KYOUNG KWAN AHN (Senior Member, IEEE) received the B.S. degree from the Department of Mechanical Engineering, Seoul National University, in 1990, the M.Sc. degree in mechanical engineering from the Korea Advanced Institute of Science and Technology (KAIST), in 1992, and the Ph.D. degree from the Tokyo Institute of Technology, in 1999.

Since 2000, he has been with the School of Mechanical Engineering, University of Ulsan, where he is currently a Professor and the Director of the Fluid Power Control and Machine Intelligence Laboratory. His main research interests include fluid based triboelectric nano generator, modeling and control of fluid power systems, energy saving construction machine, hydraulic robot, and power transmission in the ocean energy. He is the author or coauthor of over 190 SCI(E) papers and four books in these areas. He serves as an Editor for the *International Journal of Control, Automation and Systems*. He serves as an Editorial Board of renewable energy, Korean fluid power and construction machine, actuators, and so on.

• • •